A ^{1}H AND ^{13}C NMR STUDY OF MOTIONAL CHANGES OF DIPALMITOYL LECITHIN ASSOCIATED WITH THE PRETRANSITION

EDWIN BOROSKE AND LUTZ TRAHMS
Freie Universität Berlin, Institut für Atom- und Festkörperphysik, Arnimallee 14, D-1000 Berlin 33, Federal Republic of Germany

ABSTRACT Motional changes of the dipalmitoyl lecithin molecule associated with the pretransition in multibilayers are investigated by proton-enhanced ^{13}C-NMR and proton spin-locking experiments. The nitrogen-bound methyl groups of the polar head exhibit faster motion and more disorder in the intermediate phase compared with the gel phase. Although little or no change occurs in the hydrocarbon chain order at the pretransition, the corresponding motional correlation time changes by one order of magnitude. This is consistent with a model involving rotational motion of the hydrocarbon chains about their long axes: in the gel phase the motion is such that neighboring chains make an oscillating disrotatory motion, while in contrast, in the intermediate phase a quasi-free chain rotation takes place. Earlier contradicting results of Davies, J., 1979, *Biophys. J.*, 27:339–358, and ourselves, Trahms, L., and E. Boroske, 1979, *Biochim. Biophys. Acta.* 552:189–193, are explained by this model.

INTRODUCTION

Dipalmitoyl lecithin-water multibilayer systems with a water content of >20% (w/w) exhibit a well-known phase transition at $T_c \approx 42$°C that is associated with a melting of the two-dimensional lattice of the lipid bilayer and a *trans*-gauche isomerization along the hydrocarbon chains of the lecithin molecule (1–3). A pretransition at ~7°C below T_c has been detected by various methods (4–6) and crystallographically characterized (5,6). The notations $L_{\beta'}$, $P_{\beta'}$, and L_α for the gel phase ($T < 35$°C), the intermediate phase (35°C < T < 42°), and the fluid lamellar phase ($T >$ 42°C), respectively, are now commonly used.

Extensive studies using various experimental techniques were performed to elucidate the nature of the $P_{\beta'}$ phase. A rippled structure of the bilayer with periods of ~200 Å was first proposed by Tardieu et al. (5). Gebhardt et al. made extensive electron microscopic studies and found two types of ripple shapes, one symmetric and one asymmetric (7). Various proposals for the structure of the rippled $P_{\beta'}$ phase have been made (5–8). A theoretical description of the pretransition based on the Landau theory was made by Doniach (9). Recently Chan and Webb have described the intermediate phase as a martensitic structure (10).

To explain structural changes associated with the pretransition on a molecular scale, various techniques were applied. From infrared results Cameron et al. concluded that two nonequivalent hydrocarbon sites exist in the $L_{\beta'}$ phase, which become identical in the $P_{\beta'}$ phase (11, 12). In a recent x-ray study, Hentschel et al. found that the pretransition from $L_{\beta'}$ to $P_{\beta'}$ is associated with a change of the two-dimensional lattice of the hydrocarbon chains from an orthorhombic ($L_{\beta'}$) to a hexagonal ($P_{\beta'}$) structure (13, 14). This may be regarded as a confirmation of the infrared studies of Cameron et al. (11, 12). In earlier Raman experiments Gaber and Peticolas (15) found an increase in the number of gauche conformations of the hydrocarbon chains at the pretransition from the $L_{\beta'}$ to the $P_{\beta'}$ phase indicating an increase in chain disorder, which, however, has not been confirmed by recent infrared results of Cameron et al. (16) who found no significant change in the chain order at the pretransition. From electron spin resonance (ESR) saturation transfer experiments, Marsh (17) concluded an increased rotational chain motion at the pretransition from $L_{\beta'}$ to $P_{\beta'}$.

Because ESR probes always distort the lipid bilayer structure, the nonperturbing nuclear magnetic resonance (NMR) spin probes of the lipid molecule are often used to investigate its dynamic behavior. ^{2}H-NMR results reported by Füldner (18) show motional changes of the nitrogen-bound methyl groups of the polar head at the pretransition, whereas in early NMR studies of the chemical-shift tensor of ^{31}P nuclei no significant change was observed (19). Changes in the second moment of the proton NMR line of the hydrocarbon chains at the pretransition from the $L_{\beta'}$ to the $P_{\beta'}$ phase were reported earlier by us (20) and recently confirmed by a more extensive study of MacKay (21). The slight decrease of the second moment was interpreted as an increase of motional freedom. In contrast to these results, the quadrupolar second moment of deuterated hydrocarbon chains does not change at the pretransition (22). These contradictory findings lead us to question whether the decrease of the second moment of the

proton resonance is solely caused by changes of the spin-packing density or if the presumed motional changes appear only in the mean dipolar field seen by the protons and not in the deuterium quadrupolar interaction.

In the present paper we investigate both the pretransition and the main transition of dipalmitoyl lecithin by means of proton-enhanced (PE) ^{13}C-NMR as detected by delayed Fourier transformation and ^{1}H spin-locking experiments. Our analysis is, however, restricted to the pretransition. Two motionally sensitive interactions are studied. (*a*) Measurements of the cross-polarization time, T_{HC}, between the ^{1}H and ^{13}C nuclear-spin polarizations and the depolarization time, τ_D, of the ^{13}C magnetization during dipolar contact with protons have been carried out for selective studies of the time averaged local field of protons as seen by the ^{13}C nuclear spin of the hydrocarbon chains, their terminal CH_3 groups, and the N—$(CH)_3$ group of the polar head of the molecule. (*b*) The measurement of the spin-lattice relaxation time in the rotating frame, $T_{1\rho}$, have allowed partial probing of the relaxation spectrum of the hydrocarbon chains and determination of motional correlation times in the three thermotropic phases $L_{\beta'}$, $P_{\beta'}$, and L_{α}.

The results show drastic motional changes of both the head group and the hydrocarbon chains at the pretransition. While the motional change of the head group is associated with a decrease of molecular order, no significant change of the chain order occurs at the pretransition. From this we conclude that the predominant motion of the hydrocarbon chain below the main transition temperature is hindered rotation about its long axis. We propose that the orthorhombic lattice of the $L_{\beta'}$ phase corresponds to disrotatory oscillations of neighboring hydrocarbon chains by an angle of ~90°, whereas the sixfold symmetry of the hexagonal $P_{\beta'}$ structure allows quasi-free chain rotation. This model provides an interpretation of the results of the present paper and a resolution of a conflict between earlier results of ours (20) and of Davis (22).

MATERIALS AND METHODS

Protonated L, α-dipalmitoylphosphatidylcholine (L, α-DPPC) was purchased from Serva Feinbiochemica GmbH & Co. (Heidelberg, FRG) and used without further purification. Deuterated DPPC-d_{13} was synthesized by Laube (23). The samples were prepared in a spherical glass holder 9-mm diam. Thereby material was saved compared with cylindrical sample geometry and diamagnetic NMR line distortions (24) were avoided.

For preparation a branched glass tube was used (Fig. 1) containing separated reservoirs of heavy water (D_2O) and dry DPPC (D_2O/D_2O + DPPC ≈ 30% wt/wt). After filling the sample tube with nitrogen we sealed off the water branch while freezing the D_2O reservoir. To remove oxygen from the sample we repeatedly applied the following procedure: evacuation of the sample, filling with nitrogen, and thawing the D_2O reservoir. Then the D_2O reservoir was slightly heated while a weak vacuum was applied and the inlet tube above the DPPC reservoir was cooled by a pad of cotton wool previously dipped in liquid nitrogen. Thereby water was continuously distilled into the DPPC branch. The sample was then allowed to swell for two days while under nitrogen, and remainded well below the main transition temperature of T_c = 42°C. As

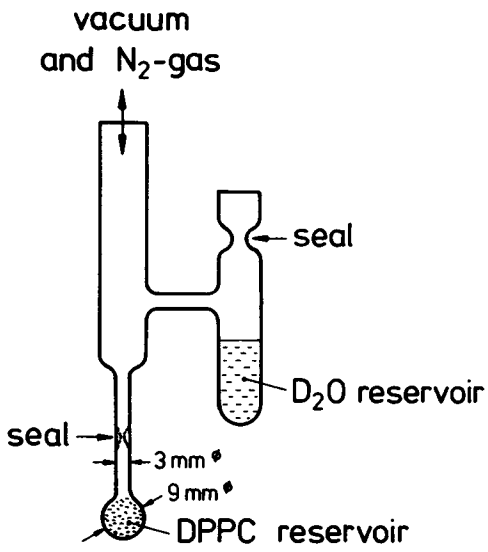

FIGURE 1 Preparation tube.

reported by Hentschel (13) this cold swelling allows homogeneous water uptake by lecithin. Then the sample was heated above T_c and again cooled. This resulted in a homogeneous and glassy lecithin-water dispersion when heated above T_c. Gas bubbles occurring in the dispersion were removed by gentle evacuation. Finally the DPPC-D_2O reservoir was sealed off leaving a short piece of the inlet tube connected with the sample holder. To keep track of the final water content we compared the initial weights of preparation tube, DPPC powder, and D_2O with the final weights of the sealed sample and the rest of the glassware.

Samples of lecithin purchased from Serva Feinbiochemica GmbH & Co. remained stable for months at 0°C with no changes in their spectra. Samples of synthesized lecithin sometimes showed drastic changes in their spectra and transition temperatures after a few days, which seemed to be caused by degradation of the molecule. The proton-enhanced ^{13}C spectra were obtained on a 300-MHz spectrometer (model CXP 300, Bruker GmbH, Karlsruhe, FRG). The frequency dependence of the proton spin-lattice relaxation time in the rotating frame, $T_{1\rho}$ was measured on a spectrometer (model SXP 4-100; Bruker GmbH), operating at 80 MHz.

RESULTS AND DISCUSSION

Competing Processes in Proton-Enhanced Nuclear Magnetic Resonance (PE-NMR) Experiments and Molecular Informations

The lecithin molecule with natural nuclear-spin abundance represents an ideal system to apply proton-enhanced nuclear magnetic resonance (PE-NMR) (25). This technique allows NMR detection of the rare ^{13}C nuclei with proton-enhanced sensitivity and spectral resolution of at least three interesting molecular fragments, namely, the hydrocarbon chains, their terminal CH_3 groups, and the N—$(CH)_3$ head group.

During the phase of polarization of the ^{13}C nuclear spins, two competing processes mainly occur, both of which yield different pieces of information about structure and dynamics of the molecule. To achieve polarization of the rare ^{13}C spins, the protons and ^{13}C nuclei are first aligned with their magnetization parallel to the fields H_{1H} and H_{1C},

which rotate with the respective Larmor frequencies, $\gamma_H H_0$ and $\gamma_C H_0$, in a plane perpendicular to the external homogeneous field, H_0. After matching their Zeeman energies in the rotating frame corresponding to the Hartman-Hahn condition (26)

$$\gamma_C H_{1C} \approx \gamma_H H_{1H}, \tag{1}$$

the dipolar coupling induces substantial cross relaxation between both spin types, which tends to enhance the ^{13}C polarization at the expense of the large proton polarization and finally equalize the inverse spin temperatures, β_H and β_C, of both spin reservoirs with a rate T_{HC}^{-1}. Provided the spin temperature concept is valid (i.e., cross relaxation has to be much faster than spin-lattice relaxation), the time evolution of the inverse spin temperature of the rare ^{13}C reservoir is approximately described by

$$\frac{\beta_C(t_C)}{\beta_H(0)} = e^{-t_C/T_{1\rho}}\,[1 - e^{-t_C(1/T_{HC} - 1/T_{1\rho})}], \tag{2}$$

where t_C is the time of dipolar contact corresponding to Eq. 1, and $T_{1\rho}$ is the spin-lattice relaxation time in the rotating frame of the proton reservoir (27). The polarization process described by Eq. 2 may be illustrated in a scheme of connected thermal reservoirs as shown in Fig. 2 *a*. The cross-polarization switch refers to the rotating frame and is closed by fulfilling Eq. 1. As the number of ^{13}C nuclei, N_C, is much smaller than the number of protons, N_H, and therefore the heat capacity of the ^{13}C spins is negligible, only one spin-lattice relaxation pathway, namely, that of the protons with the rate $T_{1\rho}^{-1}$, appears to be effective for both spin reservoirs. Eq. 2 shows that only under the condition $T_{HC}^{-1} \gg T_1^{-1}$ is substantial polarization transferred from protons to ^{13}C nuclei. The maximum value of polarization is reached at the time

$$t_m = \frac{T_{HC}}{1 - \dfrac{T_{HC}}{T_{1\rho}}} \cdot \ln \frac{T_{1\rho}}{T_{HC}}. \tag{3}$$

For times of dipolar contact much longer than t_m, the polarization enhancement is reduced to zero by the competing spin-lattice relaxation with the rate, $T_{1\rho}^{-1}$.

As cross polarization is caused by dipolar interactions between protons and ^{13}C nuclei, its rate may be expressed

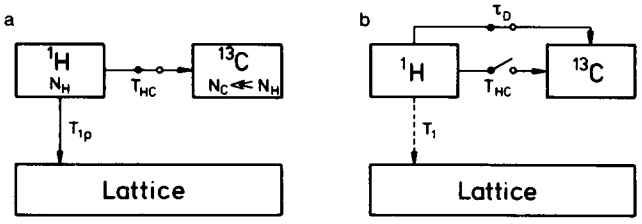

FIGURE 2 Coupled spin reservoirs of proton-enhanced ^{13}C-NMR (*a*) polarization of ^{13}C nuclei and (*b*) detection of ^{13}C magnetization by delayed Fourier transformation.

in terms of second moments. On the basis of a perturbation approach used by McArthur et al. (28), Pines et al. (25) calculated the cross polarization for the spin-locking case to be

$$T_{HC}^{-1} = C_{HC} \frac{\overline{M}_{2HC}}{\overline{M}_{2HH}^{1/2}}. \tag{4}$$

Herein $\overline{M}_{2HH}$ and $\overline{M}_{2HC}$ are the residual (i.e., partially time averaged) second moments of the proton and ^{13}C-NMR line, respectively. The dimensionless constant, C_{HC}, contains a ratio of fourth-order contributions to the internuclear dipolar coupling between protons and ^{13}C nuclei. For polycrystalline samples the second moment of the highly diluted ^{13}C nuclear spins is related to the proton second moment by

$$\overline{M}_{2HC} = \left(\frac{2}{3}\frac{\gamma_C}{\gamma_H} c_r\right)^2 \overline{M}_{2HH}, \tag{5}$$

where c_r takes into account the different spin arrangements surrounding the ^{13}C nuclei and protons, i.e., identical surroundings are characterized by $C_r = 1$. Inserting Eq. 5 into Eq. 4 we have

$$T_{HC}^{-1} = \frac{2}{3}\frac{\gamma_C}{\gamma_H} c_r \cdot C_{HC}\, \overline{M}_{2HC}^{1/2}. \tag{6}$$

Theoretically expected values of T_{HC} according to Eq. 6 are of the order of $10^{-4} - 10^{-3}$ s for a static hydrocarbon lattice with ^{13}C nuclei in natural abundance (25).

The enhanced ^{13}C magnetization may be detected by switching off the ^{13}C locking field, H_{1C}, and Fourier-transform the free induction decay (FID). If the protons are decoupled by the locking field, H_{1H}, the ^{13}C spectrum is only broadened by the chemical-shift anisotropy. The mean local proton field seen by ^{13}C nuclei is, however, directly measured by delayed Fourier transformation. This means, that the FID is transformed after switching off the proton-locking field for a period, t_D, during which the proton spins depolarize part of the ^{13}C magnetization. The depolarization pathway indicated by a closed τ_D switch in Fig. 2 *b* refers to a static internuclear spin coupling and differs physically from the cross-polarization pathway in the rotating frame. The integral intensity, $I(t_D)$, of the nondepolarized part of the ^{13}C signal decays exponentially with t_D as given by

$$I(t_D) = I_0 \cdot e^{-t_D/\tau_D}. \tag{7}$$

Actually this is in contrast to the behavior of a homogeneous spin system that exhibits a Gaussian rather than an exponential FID due to the statistical local field distribution of neighboring spins. As discussed by Abragam (29) and Mehring (27) the exponential behavior of rare spin systems is due to flip-flop motions of the abundant spins that produce partial narrowing. The relation between the

decay time and the second moment is given by

$$\tau_D^{-1} = \frac{1}{2\sqrt{3}} \left(\frac{\overline{M}_4}{\overline{M}_{2HC}^2} \right)^{-1/2} \overline{M}_{2HC}^{1/2}. \quad (8)$$

where $\overline{M}_4$ is the fourth moment of the ^{13}C-resonance line.

As both rates, τ_D^{-1} and T_{HC}^{-1}, are proportional to $\overline{M}_{2HC}^{1/2}$, they are sensitive to motional changes of the lipid molecules if the motional correlation times are $\tau_C \lesssim \overline{M}_{2HC}^{-1/2}$. The measurement of τ_D^{-1} is not perturbed by the much smaller spin-lattice relaxation rate, T_1^{-1} (dotted pathway in Fig. 2 *b*), which corresponds to the high static field, H_0. However, during the polarization phase the rate of proton spin-lattice relaxation in the rotating frame, $T_{1\rho}^{-1}$, corresponds to the low rotating field, H_{1H}, and it may therefore compete with T_{HC}^{-1} as Eq. 4 takes into account. An extensive study of spin-lattice relaxation in the rotating frame due to random molecular motion was made by Haeberlen and Waugh (30). For the resonant spin-locking case they derived

$$T_{1\rho}^{-1} = \overline{M}_{2HH} \frac{\tau_C}{1 + 4\omega_1^2 \tau_C^2}, \quad (9)$$

where $\omega_1 = \gamma H_{1H}$ is the Zeeman frequency of the proton spins with respect to the rotating field, H_{1H}, and the second moment, $\overline{M}_{2HH}$, represents the mean-square amplitude of the dipolar relaxation field. Actually Eq. 9 is valid only if the correlation time $\tau_C \gtrsim 1/\omega_0$, neglecting the small contributions of the relaxation spectrum near the Zeeman frequency in the laboratory frame, ω_0. For frequencies of 300 MHz used in our experiments, this corresponds to $\tau_C \gtrsim 10^{-9}$ s. As reviewed by Charvolin and Tardieu (31) characteristic time constants of lipids in the L_α phase due to lateral diffusion and reorientation of the hydrocarbon-chain axis are of the order of 10^{-8} s. Furthermore, motional freedom is strongly restricted in the crystalline $L_{\beta'}$, and $P_{\beta'}$ phases of lecithin and we may assume that Eq. 9 is valid for lecithin double layers.

As seen from Eq. 9 the relaxation spectrum may be probed at a constant static field, H_0, by varying the locking field, H_{1H}. If motions with characteristic times, $\tau_C \sim 1/\omega_1$, are present, the correlation time is determined from the point of maximum slope of the relaxation spectrum by $\tau_C = (\sqrt{2})/(6 \cdot \omega_{1max})$. Additional temperature variation may allow determination of the temperature dependence of τ_C. Owing to experimental limitations on locking fields and the spin-locking condition, $\gamma H_1 \gtrsim M_{2HH}^{1/2}$, for satisfactory quantization fields in the rotating frame, this probing technique covers a time range between 10^{-4} and 10^{-6} s.

In this section we discussed the rate processes involved in PE-NMR experiments with respect to interesting molecular parameters, namely, the second moments of the abundant proton, the rare ^{13}C-nuclear spins, $\overline{M}_{2HH}$ and $\overline{M}_{2HC}$, and the characteristic times of molecular motion, τ_C. The overall dynamic range of the method allows studies of molecular motion that is most sensitive in a time window from 10^{-3} to 10^{-6} s.

Features of Proton-Enhanced ^{13}C Spectra

In Fig. 3 proton-enhanced spectra of a DPPC-water dispersion (D_2O content: 30% wt/wt) representative for the gel ($L_{\beta'}$), the intermediate ($P_{\beta'}$), and the fluid (L_α) phase are shown. In all three phases the CH_2 chains, the terminal CH_3 groups and the N-$(CH_3)_3$ groups of the polar head are fairly well resolved. The best resolution, owing to lower molecular order and motional narrowing, is achieved in the fluid L_α phase. Only in this phase does the —C═O position exhibit detectable polarization enhancement. This indicates that in the less ordered L_α phase, the dipolar contact of the —C═O group with protons in its intra- or intermolecular neighborhood is substantial, whereas there is less contact in the intermediate and in the gel phase, where the chains are assumed to be in the relatively stiff all-*trans* configuration.

By further comparison of the spectra, two remarkable features appear (*a*) the chosen contact time, $t_C = 20$ ms, is near the optimum time, t_m, for the hydrocarbon region, i.e., the CH_2 chain and its terminal CH_3 group in the gel $L_{\beta'}$ as well as in the fluid L_α phase, whereas in the intermediate $P_{\beta'}$ phase the polarization of this region is almost completely destroyed by spin-lattice relaxation. This indicates that the spin-lattice relaxation time, $T_{1\rho}$, must be consider-

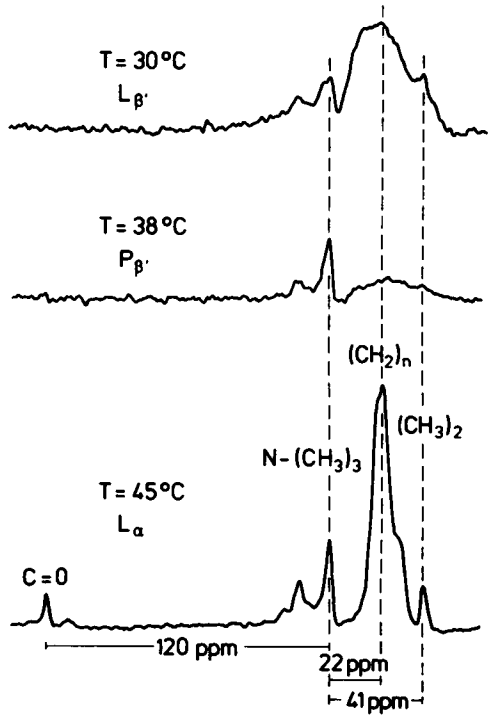

FIGURE 3 Proton-enhanced spectra of a DPPC-D_2O dispersion (D_2O content 30% wt/wt). The ^{13}C nuclear magnetization was detected after polarization contact of t_C = 20 ms.

ably lower in the $P_{\beta'}$ phase than in the $L_{\beta'}$ phase and motional changes of the hydrocarbon chain appear at the pretransition. (*b*) While the linewidth of the hydrocarbon region does not measurably change at temperatures below the main transition, a quite different behavior is observed for the N—$(CH_3)_3$ signal. It shows nearly the same linewidth in the $P_{\beta'}$ and the L_α phase, whereas in the gel phase a broadening occurs. This indicates an increase of disorder in the head-group region but no measurable change of chain order at the pretransition from the gel to the intermediate phase.

Time Constants T_{HC}, τ_D, and $T_{1\rho}$

For a deeper understanding of the spectral features mentioned above we now look systematically at the temperature dependences of the time constants T_{HC}, $T_{1\rho}$, and τ_D. T_{HC} and $T_{1\rho}$, which differ by at least one order of magnitude, could be determined from the dependency of the integral line intensities on the contact time, t_C by fitting Eq. 2 to the experimental points. The time constant of the decay of the integral intensity, τ_D, was determined by means of Eq. 7. The times, T_{HC} and τ_D, mainly contain the residual second moment due to the effective proton field seen by ^{13}C nuclei. They will therefore be discussed in connection with each other. As shown in Fig. 4 both T_{HC} and τ_D of the CH_2 chains exhibit a small step at the pretransition and a change of about one order at the main transition temperature, T_C. The relative changes of T_{HC} and τ_D at both transitions are of same size and also in good agreement with our earlier results (20) and recent experiments of MacKay (21).

Owing to the lower local field at the terminal CH_3 position, the absolute values of the corresponding time constants, T_{HC} and τ_D, are in all phases larger than those of the CH_2 chain. However, their relative changes compared with those observed for the CH_2 chains are of the same order at the pretransition but larger at the main transition. This indicates that changes of the motional structure occurring at the pretransition have the same character for both molecular parts, namely, the CH_2 chain and its terminal CH_3 group. It seems therefore unlikely that the pretransition is associated with a chain end melting and decoupling of the monolayers as was speculated earlier (20, 32). These results further indicate a higher disorder of the CH_3 chain end compared with the CH_2 chain in the fluid L_α phase, a fact that is well known from very early deuterium NMR experiments (2).

In contrast to the behavior of the chain region, the N—$(CH_3)_3$ head group shows a drastic relative change of τ_D at the pretransition and a much smaller one at the main transition. This result is in accordance with the observation of line narrowing of the N—$(CH_3)_3$ signal at the pretransition from the $L_{\beta'}$ to the $P_{\beta'}$ phase and may be interpreted as a decrease of the molecular order parameter of the head group. Most likely the N—$(CH_3)_3$ end of the polar head undergoes substantial structural change with respect to motion and molecular order at the pretransition. Earlier results of Brown and Seelig (19) did not exhibit changes in the ^{31}P chemical-shift tensor at the pretransition. One may therefore conclude from the present results that in the intermediate phase the polar head is much less ordered at the choline end than near the glycerol backbone of the molecule.

So far the data of T_{HC} and τ_D for the chain region do not allow us to decide whether the observed changes are of geometrical or dynamic origin. It may, however, be concluded from the constant line width observed for the ^{13}C

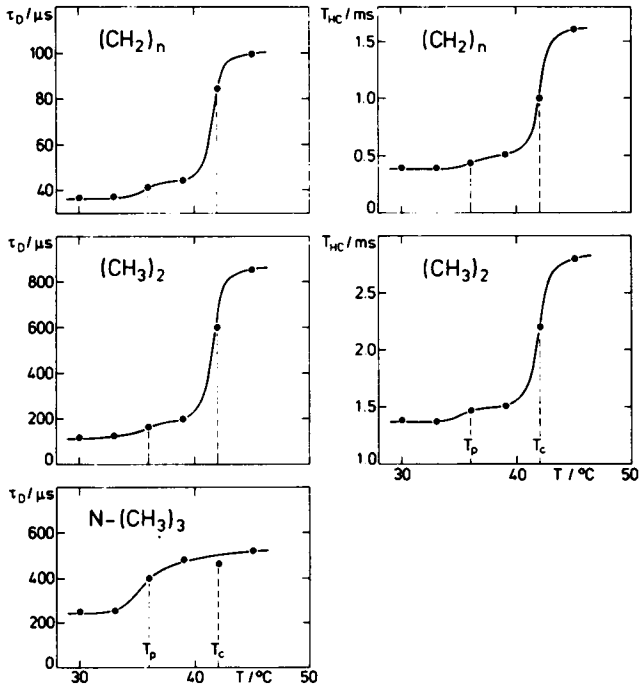

FIGURE 4 Temperature dependences of τ_D and T_{HC} with respect to the molecular fragments $(CH_2)_n$, $(CH_3)_2$, and N—$(CH_3)_3$.

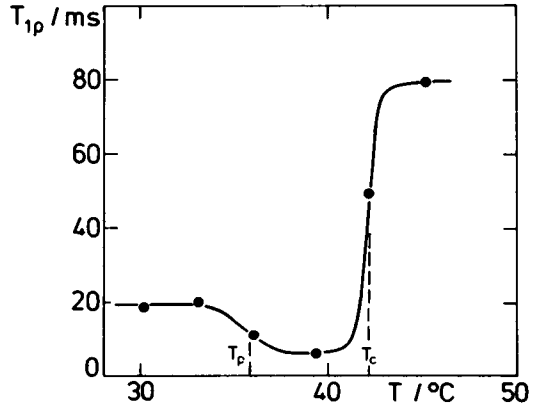

FIGURE 5 Temperature dependence of the proton spin-lattice relaxation time in the rotating frame, $T_{1\rho}$, of the whole DPPC molecule.

chain signals in the $L_{\beta'}$ and $P_{\beta'}$ phase that if there is any motional change associated with the pretransition, it must not change the chain order. Direct information about dynamic changes at the pretransition is obtained from the temperature dependence of the spin-lattice relaxation times in the rotating frame, $T_{1\rho}$, shown in Fig. 5. Whereas the times, T_{HC} and τ_D, always increase with temperature, i.e., parallel with presumed molecular motion, $T_{1\rho}$ shows its minimum values in the intermediate phase. It decreases discontinuously by a factor of 2.5 at the pretransition but increases again by one order at the main transition. This indicates a drastic change by a factor of 2.5 or more of the motional correlation time, τ_C, at the pretransition and a change of at least one order at the main transition. For an estimate of τ_C one may assume the time constant, $T_{1\rho}(\tau_C)$, according to Eq. 9 to have its minimum value just in the intermediate phase, where $\tau_C = 1/2\omega_1$. Using the experimental value of $\omega_1 = \gamma H_1 \approx 2 \cdot 10^5$ rad/s this estimate yields $\tau_C \approx 2.5 \cdot 10^{-6}$ s. This shows unambiguously that the molecular changes of the chain region at the pretransition appearing in small but measurable discontinuties of T_{HC} and τ_D as well as in second moments are of dynamic origin. Furthermore, these dynamic changes occur without variation of the intramolecular chain order, i.e., without variation of the number of degrees of motional freedom.

Determination of Motional Correlation Times τ_C

As shown in the preceding section, the molecular motion in the $P_{\beta'}$ phase occurs with correlation times of the order of 10^{-6} s. This offers the chance of probing the proton relaxation spectrum and of determining the related correlation times in the various thermotropic phases by spin-locking experiments by simply measuring the exponential time decay of the locked proton magnetization. Since ω_1 was restricted between 10^5 and $3 \cdot 10^5$ rad/s by our experimental set up and by the spin-locking condition, we could not expect to determine τ_C in all phases directly from the maximum slope of the relaxation spectrum. Nevertheless this small spectral window was promising to permit observation of the temperature dependence of relaxation of the chain protons. Fig. 6 shows the temperature dependence of $T_{1\rho}$ for four equidistant proton-locking fields measured on partially deuterated DPPC-d_{13}. All curves exhibit a distinct step at the pretransition and a much larger one of opposite sign at the main transition. In the $L_{\beta'}$ phase the relative variation of the relaxation time with frequency decreases with increasing ω_1. Almost no relative variation of $T_{1\rho}$ with ω_1 is, however, observed in the L_α phase. This may be quantitatively discussed by $T_{1\rho}^{-1}$ as a function of ω_1 as illustrated in Fig. 7. The three curves correspond to the temperatures 30, 39, and 43.5°C, which represent the phases $L_{\beta'}$, $P_{\beta'}$, and L_α, respectively. Unfortunately the available frequency window allows direct determination of τ_C only in the intermediate phase, where a

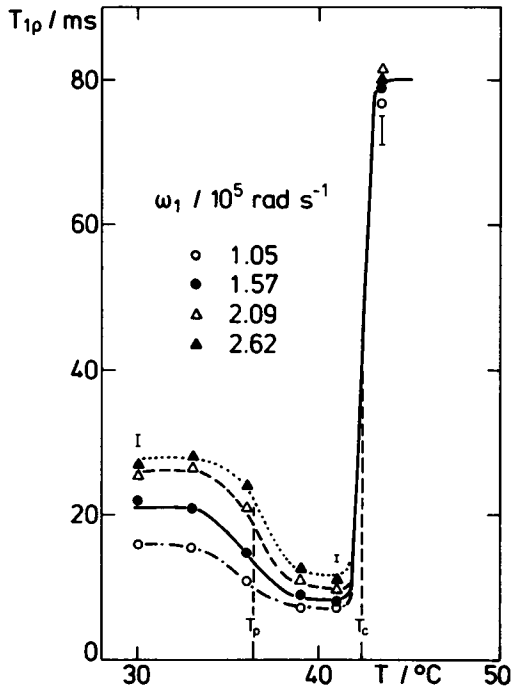

FIGURE 6 Temperature dependence of $T_{1\rho}$ of the hydrocarbon chains at four equidistant proton-locking fields, $H_{1H} = \omega_1/\gamma$.

reliable least-square fit according to Eq. 9 is possible owing to the observed variations of $T_{1\rho}(\omega_1)$ around the point of maximum slope. The fit yields $\tau_C(P_{\beta'}) = 1.8 \cdot 10^{-6}$ s. In the fluid L_α phase one evidently observes the low frequency part of the relaxation spectrum, where $4\omega_1^2\tau_C^2 \ll 1$. In this limiting case $T_{1\rho}^{-1}$ is approximately constant and given by

$$T_{1\rho}^{-1} \approx \overline{M}_{2HH}\, \tau_C(L_\alpha). \qquad (10)$$

Taking $\overline{M}_{2HH} \approx 10^8$ s^{-2} from earlier results (20) we estimate $\tau_C(L_\alpha) \approx 10^{-7}$ s. As recently reported by Van der

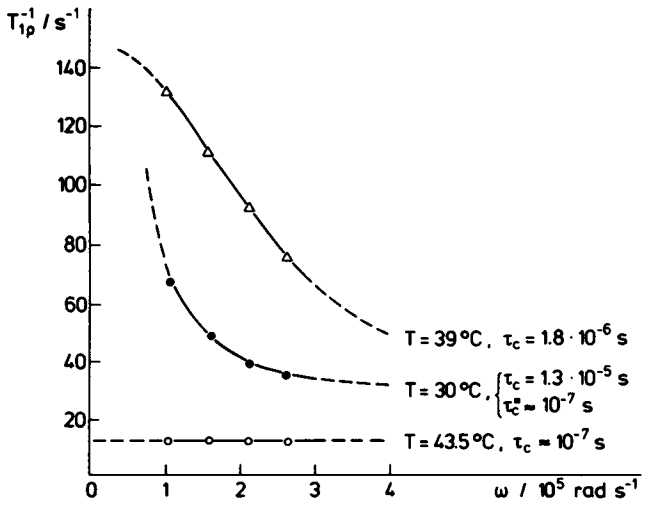

FIGURE 7 Relaxation spectra of the hydrocarbon chains at temperatures representative for the phases $L_{\beta'}$ (30°C), $P_{\beta'}$ (39°C), and L_α (43.5°C).

Leeuw and Stulen (33), two independent correlation times of the orders 10^{-7} and 10^{-9} s occur in the L_α phase of lecithin. These refer to reorientation of the hydrocarbon chain and rotation about the chain axis, respectively. The value estimated in the present work presumably corresponds to the slower motion of chain-axis reorientation.

In contrast to its behavior in the L_α phase, the relaxation spectrum monitored in the $L_{\beta'}$ phase appears with its high frequency tail in our probing window. Owing to an additional constant contribution to the relaxation rate, this spectrum cannot be fitted according to Eq. 9. Evidently this spectrum is a superposition of two spectra, one occurring with its high frequency tail ($4\omega_1^2\tau_C^2 \gg 1$) and the other with its constant low frequency part, $\overline{M}_{2HH}\tau_C^*$. The relaxation rate as a function of ω_1 is then approximated by

$$T_{1\rho}^{-1}(\omega_1) = \overline{M}_{2HH}\left(\tau_C^* + \frac{1}{\tau_C}\omega_1^{-2}\right). \qquad (11)$$

A least-square fit directly yields $\tau_C = 1.3 \cdot 10^{-5}$ s corresponding to the slower motion, whereas the correlation time of the fast motion is estimated to be $\tau_C^* \approx 10^{-7}$ s.

Model of the Hydrocarbon-Chain Structure

In the present paper we used the wide dynamic range of proton-enhanced ^{13}C-NMR to study motion of the lecithin molecule below the main transition temperature. As mentioned in the Introduction the bilayer structure in the phases $L_{\beta'}$ and $P_{\beta'}$ is characterized by a two-dimensional lattice of the hydrocarbon chains of the lecithin molecule, which are assumed to exist preferentially in an all-*trans* configuration. Therefore, we interpret our results in a structural model with respect to the hydrocarbon-chain region of the molecule. In the results of section Determination of Motional Correlation Times τ_C it is shown that even in the crystalline phases $L_{\beta'}$ and $P_{\beta'}$ significant motion of the hydrocarbon chains exists. The corresponding correlation times in the range of 10^{-5} to 10^{-7} s are short enough to cause partial motional narrowing of the dipolar broadened NMR lines. If we assume an all-*trans* configuration of the chains, the low values of experimentally found second moments, $\overline{M}_{2HC}$ and $\overline{M}_{2HH}$, compared with the static second moments (the present work and references [20] and [21]) suggest rotation as the major narrowing motion in the $L_{\beta'}$ and $P_{\beta'}$ phases. This assumption will be quantitatively discussed on the basis of model calculations in the accompanying publication (34).

We also observed a drastic change in the correlation time by about one order at the pretransition associated with a small change in the dipolar second moment, $\overline{M}_{2HC}$, of ~30%. No measurable change of the decoupled ^{13}C-NMR line width was observed, indicating a lack of measurable change of the chain order at the pretransition. Therefore, we again may assume rotation around the long chain axis as the dominating kind of motion in the $L_{\beta'}$ and $P_{\beta'}$ phases. For a detailed discussion of motion in connection with molecular structure we now refer to x-ray studies of Hentschel et al. (13, 14), where an orthorhombic and a hexagonal lattice were assigned to the $L_{\beta'}$ and $P_{\beta'}$ phases, respectively.

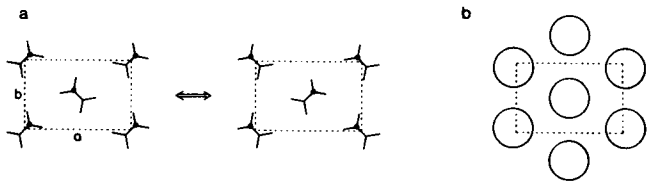

FIGURE 8 Two-dimensional hydrocarbon lattice of the lecithin bilayer (*a*) orthorhombic ($L_{\beta'}$) and (*b*) hexagonal ($P_{\beta'}$).

In Fig. 8 *a* two alternative structures of an idealized orthorhombic lattice are illustrated by cross sections perpendicular to the hydrocarbon-chain axes. The projections of the chemical bonds onto the sectional area are indicated by drawn lines. Carbon atoms, which are located in the sectional area, are marked by points. The orientation of the chains is defined by the position of the C—C bonds onto the sectional area. Although we do not believe these idealized structures exist in the bilayer, simple sterical arguments suggest preferential orientation of the C—C bonds around the two alternative positions illustrated in Fig. 8 *a*. Since the deviation of the orthorhombic lattice from a hexagonal symmetry is small, thermally activated disrotatory oscillations between the alternative structures seem possible. This implies a restricted correlated chain rotation, where neighboring chains are geared into each other analogous to a cog-wheel drive. A similar kind of motion was proposed by Kozelj et al. for a crystalline phase of the system $(C_{10}H_2NH_3)_2CuCl_4$ (35). From the short motional correlation times of 10^{-5} to 10^{-7} s found for the $L_{\beta'}$ phase (Results: Determination of Motional Correlation Times τ_C), we may then conclude that this flip-flop motion

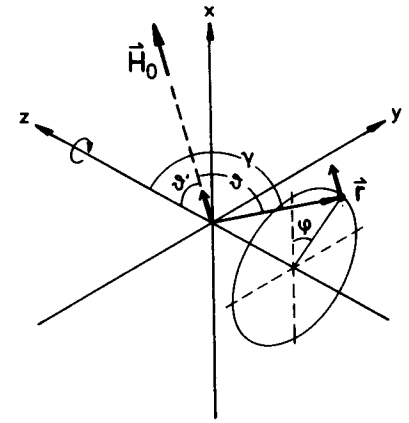

FIGURE 9 Spin pair of distance r quantized in a field, H_0, and rotated around the *z*-axis.

occurs in the fast limit with respect to the nuclear dipolar interactions (i.e., $\tau_C \ll \overline{M}_2^{-1/2}$). The hexagonal lattice found for the $P_{\beta'}$ phase has a slightly lower molecular packing density than the orthorhombic structure. It allows a sixfold hindered rotation of a hydrocarbon chain independent of its neighbors, which in the fast limit is equivalent to free rotation. From the correlation time of the order 10^{-6} s, we again conclude the fast limit to exist in the $P_{\beta'}$ phase. In Fig. 8 *b* we have indicated this motional state simply by circles about the centers of the chains.

We are now in a position to test the proposed model by consistent interpretation of the present results on the basis of a detailed analysis of the chain oscillation and free rotation and its influences on dipolar second moments. To discuss the intrachain part of the dipolar second moment, we regard one interacting spin pair of distance **r** quantized in a field $\mathbf{H}_0$ using a representation in accordance with that of Andrew (36) as illustrated in Fig. 9. Its contribution to the second moment is proportional to $\langle 3\cos^2\theta - 1\rangle^2$, where the time average has to be taken before the square. To find out the difference in motional averaging caused by the two proposed kinds of motion, i.e., oscillation and free rotation, we express the dependence of the second moment contribution on θ by the angles θ', γ, and ϕ in a coordinate system with respect to the rotation axis (z-axis) of the spin pair as given by

$$\begin{aligned}(3\cos^2\theta - 1) = {} & 3(\sin\theta'\sin\gamma)^2\cos^2\phi \\ & + 6(\sin\theta'\cos\theta'\sin\gamma\cos\gamma)\cos\phi \\ & + 3(\cos\theta'\cos\gamma)^2 - 1.\end{aligned} \tag{12}$$

The constant angles θ' between z-axis (rotation axis) and the field vector, $\mathbf{H}_0$, and γ between the z-axis and the spin distance vector, **r**, are defined in accordance with a treatment of rotational averaging by Abragam (29), whereas the variable angle, ϕ, describes the actual orientation of the spin distance vector **r**. The field **H** is chosen to lie in the x–z plane.

To simplify the discussion we assume a rotation angle between the two alternating positions of the oscillation of $\pi/2$. This approximation is allowed because small deviations from $\pi/2$ occur as second-order corrections in the average of Eq. 12. Under this assumption four physically interesting cases that show equivalent motional averaging of the oscillation and free rotation due to the vanishing second term in Eq. 12 are given by the combinations

$$\gamma = \frac{\pi}{2},\ \theta' : \text{arbitrary} \tag{13a}$$

$$\gamma = 0,\ \theta' : \quad '' \tag{13b}$$

$$\theta' = \frac{\pi}{2},\ \gamma : \quad '' \tag{13c}$$

$$\theta' = 0,\ \gamma : \quad ''. \tag{13d}$$

A general discussion of the interchain contribution to the dipolar second moment becomes more complicated as the time average has to be taken into account not only with respect to the angle, θ, but also with respect to the spin distance, r. It may, however, be seen from simple geometric arguments that in a rectangular symmetry (e.g., Fig. 8 *a*), a $0 - \pi/2$ flip-flop motion may reduce the interchain dipolar second moment at maximum by a factor of two. In contrast to this, free rotation results in a large reduction of the mean interchain spin distance and the interchain contributions to the dipolar second moment become negligibly small.

The model of the hydrocarbon-chain structure is now presented in detail. On its basis we may predict that according to Eq. 13a the contributions of the CH_2 proton pair to the second moments, $\overline{M}_{2HH}$ and $\overline{M}_{2HC}$, of the proton and the ^{13}C-NMR line remain constant at the pretransition. A further term to $\overline{M}_{2HH}$, which according to Eq. 13b is expected to be constant at the pretransition, is due to dipolar interaction of a proton with its nearest neighbors along the chain-axis direction. Due to the short interspin distance these intrachain interactions dominate the second moments, $\overline{M}_{2HH}$ and $\overline{M}_{2HC}$. From this we expect small relative changes of $\overline{M}_{2HH}$ and $\overline{M}_{2HC}$ at the pretransition. An important origin of the decrease of the second moment observed at the pretransition from the $L_{\beta'}$ to the $P_{\beta'}$ phase may be the onset of a quasi-free chain rotation in the $P_{\beta'}$ phase that reduces the interchain part of the second moment to negligible values. As a matter of course the large change of the correlation time observed at the pretransition is not expected to appear in $\overline{M}_{2HH}$ and $\overline{M}_{2HC}$ as long as the time average refers to the fast limit of motion that is assumed to exist in both the $L_{\beta'}$ and the $P_{\beta'}$ phases.

With this model we may interpret earlier results of Davis (22), which appear contradictory to ours (20), and those of MacKay (21). The results of Davis show that partial averaging due to fast motion exists in the $L_{\beta'}$ and $P_{\beta'}$ phases, but no change of the total quadrupolar second moment of the hydrocarbon chain is observed at the pretransition. If small deviations from axial symmetry are neglected, quadrupole interaction is analog to dipolar interaction and its rotational averaging can be described by means of Eq. 12. Since the quadrupole tensor of a C—D bond is oriented perpendicular to the hydrocarbon-chain axis, it corresponds to Eq. 13a. Therefore, changes of the quadrupolar second moment are not expected.

Finally we emphasize that our discussion refers to the overwhelming number of the molecules, i.e., those belonging to the two-dimensional lattice. The observation of a second signal with a smaller second moment in the $P_{\beta'}$ phase (37–39) indicates some kind of inhomogeneities in the sample, where molecules diffuse with lower order than within the two-dimensional lattice. As this onset of low-order diffusion is already observed at 27°C, well below the pretransition temperature of 35°C, we do not believe that it is related to the discontinuities of the proton second

moments and motional correlation times at the pretransition temperature.

The authors wish to thank Professor W. Helfrich for helpful discussions. We are also grateful to T. Laube and Professor H. Kurreck for synthesis of partially deuterated DPPC-d_{13}. The experimental support by Dr. Förster of Bruker GmbH, Karlsruhe, is gratefully acknowledged.

This research was supported by the Deutsche Forschungsgemeinschaft.

Received for publication 1 April 1982 and in final form 23 December 1982.

REFERENCES

1. Chapman, D., R. M. Williams, and B. D. Ladbrooke. 1967. Physical studies of phospholipids. IV. Thermotropic and lyotropic mesomorphism of some 1,2 diacyl-phosphatidylcholines (lecithins). *Chem. Phys. Lipids.* 1:445–475.
2. Seelig, J., and W. Niederberger. 1974. Two pictures of a lipid bilayer. A comparison between deuterium label and spin-label experiments. *Biochemistry.* 13:1585–1588.
3. Hinz, H. T., and J. H. Sturtevant. 1972. Calorimetric studies of dilute aqueous suspensions of bilayers formed from synthetic L-α-lecithins. *J. Biol. Chem.* 247:6071–6075.
4. Ladbrooke, B. D., and D. Chapman. 1969. Thermal analysis of lipids, protein and biological membranes. A review and summary of some recent studies. *Chem. Phys. Lipids.* 3:304–356.
5. Tardieu, A., V. Luzatti, and F. C. Reman. 1973. Structure and polymorphism of the hydrocarbon chains of lipids: A study of lecithin-water phases. *J. Mol. Biol.* 75:711–733.
6. Janiak, M. J., D. M. Small, G. G. Shipley. 1976. Nature of the thermal pretransition of synthetic phospholipids: Dimyristoyl- and dipalmitoyllecithin. *Biochemistry.* 15:4575–4580.
7. Gebhardt, C., H. Gruler, and E. Sackmann. 1977. On domain structure and local curvature in lipid bilayers and biological membranes. *Z. Naturforsch. Sect. C. Biosci.* 32:581–596.
8. Larsson, K. 1977. Folded bilayers–an alternative to the rippled lamellar lecithin structure. *Chem. Phys. Lipids.* 20:225–228.
9. Doniach, S. 1979. A thermodynamic model for the monoclinic (ripple) phase of hydrated phospholipid bilayers. *J. Chem. Phys.* 70:4587–4596.
10. Chan, W. K., and W. W. Webb. 1980. Possible martensitic transformation in hydrated phospholipid liquid crystals. *Phys. Rev. Lett.* 46:39–42.
11. Cameron, D. G., H. L. Casal, E. F. Gudgin, and H. H. Mantsch. 1980. The gel phase of dipalmitoyl phosphatidylcholine and infrared characterization of the acyl chain packing. *Biochim. Biophys. Acta.* 596:463–467.
12. Cameron, D. G., H. L. Casal, and H. H. Mantsch. 1980. Characterization of the pretransition in 1,2-dipalmitoyl-sn-glycero-3-phosphocholine by Fourier-transform infrared spectroscopy. *Biochemistry.* 19:3665–3672.
13. Hentschel, M. 1981. Ph.D. dissertation. Röntgenstrukturuntersuchungen von orientierten Lecithin-Vielschichtsystemen. Freie Universität, Berlin.
14. Hentschel, M., R. Hosemann, and W. Helfrich. 1980. Direct x-ray study of the molecular tilt in dipalmitoyl lecithin bilayers. *Z. Naturforsch. A.* 35:643–644.
15. Gaber, B. P., and W. L. Peticolas. 1977. On the quantitative interpretation of biomembrane structure by Raman spectroscopy. *Biochim. Biophys. Acta.* 465:260–274.
16. Cameron, D. G., H. L. Casals, and H. H. Mantsch. 1981. The thermotropic behavior of dipalmitoyl phosphatidylcholine bilayers. A Fourier transform infrared study of specifically labeled lipids. *Biophys. J.* 35:1–16.
17. Marsh, D. 1980. Molecular motion in phospholipid bilayers in the gel phase: long axis rotation. *Biochemistry.* 19:1632–1637.
18. Füldner, H. H. 1980. Ph.D. dissertation. Molekulare Ordnungen in reinen Lipid- und Lipid-Protein-Modellmembranen. Universität Ulm.
19. Brown, M. F., and J. Seelig. 1978. Influence of cholesterol on the polar region of phosphatidylcholine and phosphatidylethanolamine bilayers. *Biochemistry.* 17:381–384.
20. Trahms, L., and E. Boroske. 1979. Pulse NMR study of phase transitions in dipalmitoyl phosphatidylcholine multibilayers systems. *Biochim. Biophys. Acta.* 552:189–193.
21. MacKay, A. L. 1981. A proton NMR moment study of the gel and liquid-crystalline phases of dipalmitoyl phosphatidylcholine. *Biophys. J.* 35:301–313.
22. Davis, J. H. 1979. Deuterium magnetic resonance study of the gel and liquid crystalline phases of dipalmitoyl phosphatidylcholine. *Biophys. J.* 27:339–358.
23. Laube, T. 1980. Diploma work. Synthese und spektroskopische Charakterisierung spezifisch deuterierter 3-sn- und 2-Phosphatidylcholine (*L*-α- und β-Lecithine). Freie Universität Berlin.
24. Höffken, W. 1981. Diploma work. Diamagnetische Effekte auf NMR-Linienformen in magnetisch inhomonenen Systemen, gezeigt am Beispiel von Lecithin-Wasser Systemen. Freie Universität Berlin.
25. Pines, A., M. G. Gibby, and J. S. Waugh. 1973. Proton enhanced NMR of dilute spins in solids. *J. Chem. Phys.* 59:569–589.
26. Hartmann, S. R., E. L. Hahn. 1962. Nuclear double resonance in the rotating frame. *Phys. Rev.* 128:2042–2053.
27. Mehring, M. 1976. NMR Basic Principles and Progress. Vol. 11. P. Diehl, E. Fluck, and R. Kosfeld, editors. Springer-Verlag, Berlin-Heidelberg-New York.
28. McArthur, D. A., E. L. Hahn, and R. E. Walstedt. 1969. Rotating-frame nuclear-double-resonance dynamics: Dipolar fluctuation spectrum in CaF_2. *Phys. Rev.* 188:609–638.
29. Abragam, A. 1961. The Principles of Nuclear Magnetism. N. F. Mott, E. C. Bullard, and D. H. Wilkinson, editors. Oxford University Press, London.
30. Haeberlen, U., and J. S. Waugh. 1969. Spin-lattice relaxation in periodically perturbed systems. *Phys. Rev.* 185:420–429.
31. Charvolin, J., and A. Tardieu. 1978. Lyotropic liquid crystals: structures and molecular motions. *Solid State Phys.* 14(Suppl.):209–257.
32. Helfrich, W. 1976. Defect model of the solid-to-smectic B phase transition. *Phys. Lett. A.* 58:457–458.
33. Van der Leeuw, Y. C. W., and G. Stulen. 1981. Proton relaxation measurements on lipid membranes oriented at the magic angle. *J. Magn. Reson.* 42:434–445.
34. Trahms, L., W. Klabe, and E. Boroske. 1983. ^{1}H-NMR study of the three low temperature phases of DPPC-water systems. *Biophys. J.* 42:285–293.
35. Kozelj, M., V. Rutar, T. Zupancic, and R. Blinc. 1981. ^{13}C NMR study of the "bilayer" phase transitions in $(C_{10}H_{21}NH_3)_2CuCl_4$. *J. Chem. Phys.* 74:4123–4129.
36. Andrew, E. R. 1950. Molecular motion in certain solid hydrocarbons. *J. Chem. Phys.* 18:607–618.
37. Wittebort, R. J., C. F. Schmidt, and R. E. Griffin. 1981. Solid-state carbon-13 nuclear magnetic resonance of the lecithin gel to liquid-crystalline phase transition. *Biochemistry.* 20:4223–4228.
38. Wittebort, R. J., A. Blume, T. -H. Huang, S. K. Das Gupta, and R. G. Griffin. 1982. Carbon-13 nuclear magnetic resonance investigations of phase transitions and phase equilibria in pure and mixed phospholipid bilayers. *Biochemistry.* 21:3487–3502.
39. Cornell, B. A. 1981. The effect of the bilayer phase transition on the carbonyl carbon-13 chemical shift anisotropy. *Chem. Phys. Lipids.* 28:69–78.